

Spin nutation and polarization in ballistic semiconductor nanostructures

Sam Young Cho*

*Centre for Modern Physics and Department of Physics, Chongqing University, Chongqing 400044, People's Republic of China
and Department of Physics, The University of Queensland, 4072, Australia*

(Received 1 May 2008; revised manuscript received 2 June 2008; published 30 June 2008)

The definitions of spin orientation and polarization vectors are introduced within the particle density matrix of scattering states in leads. It is shown that spin-density vector can be defined by the product of the spin orientation vector, being a unit direction vector, and the charge density, corresponding to the amplitude of the spin-density vector, experimentally observable by a spatial charge modulation measurement. When an electron transports through a ballistic semiconductor nanostructure, due to quantum interference of two spin eigenmodes, the electron spin generally undergoes *nutation* on its precession around the effective magnetic field resulting from spin-orbit interactions. The nutation of electron spin is found to be crucial for spin polarization in the quantum transport. When one of two spin-dependent channels in leads is evanescent, electron spin is shown to be fully polarized for distance from the interface larger than the spin precession length.

DOI: [10.1103/PhysRevB.77.245326](https://doi.org/10.1103/PhysRevB.77.245326)

PACS number(s): 73.23.Ad, 72.25.Dc, 71.70.Ej, 72.25.Mk

I. INTRODUCTION

Recent advances in nanotechnology have made it possible to transport electron spin coherently over hundreds of micrometers at low temperature.¹ It may enable the realization of quantum spintronics^{2–4} by manipulating the spin degree of freedom of electrons without destroying their phase coherence. A spin-dependent transport has been studied in the context of the Aharonov-Casher phase^{5–8} and spin Berry phase.^{9–12} Various types of interesting phenomena have been found in spin transport systems. Examples include the spin transistor effect,¹³ spin precession in two-dimensional systems,^{14–17} spin conductance,^{18–20} spin polarization,^{21,22} spin current in mesoscopic rings with spin-orbit (SO) interactions,²³ entanglement,^{24,25} spin separation in a two-dimensional hole gas,²⁶ and spin Hall effect.^{27–31}

For various types of spintronic devices,^{2,32–42} the ballistic spin transport has been studied because it can be manipulated via SO interactions. Since SO interactions are a relativistic effect when the electron-spin experiences an effective magnetic field when it is moving through an electric field, the SO interactions can be tuned by an applied electric field in nanoscale transport devices. Indeed, in a two-dimensional electron gas system, the Rashba SO interaction^{43,44} arises due to the inversion asymmetry of the quantum well. The asymmetry of the quantum well potential can be controlled by an applied gate voltage perpendicular to the well. Also, a crystal inversion asymmetry in the devices gives rise to another type of SO interaction which is called the Dresselhaus SO interaction.⁴⁵ Such asymmetries will lift the electron-spin degeneracy and create spin-split energy bands even when no external magnetic field is applied. The spin-split energy bands can make the electron-spin precess and polarize when it travels through the quantum devices with SO interactions. Then, spatial spin dynamics due to the SO interactions is important in understanding spin polarization in ballistic quantum devices.

To study various ballistic spin transport phenomena, wave function approaches^{34–37,46} within the scattering matrix formalism, and Green's function techniques^{30,32,33} with discrete

lattices have been used in quasi-one-dimensional systems. As another way, in Ref. 18, spin-density matrix based on scattering matrix has been employed to investigate decoherence of transported spin in multichannel systems with SO interactions. Reference 18 also introduced a spin-polarization vector in terms of scattering matrix amplitudes. In this paper, we will investigate spatial electron-spin dynamics when electron spins pass through a quantum device with spin-splitting bands. A particle density matrix from the eigenfunctions of a system Hamiltonian is introduced to study coherent electron-spin transport through ballistic quantum devices. The particle density matrix is to be the product of the charge-density and spin-density matrix. The spin orientation and polarization vectors can be defined from the spin-density matrix. The spin orientation and polarization are expressed in terms of the charge density and the spin-density vector. It is found that, generally, spin splitting of electron bands in leads gives rise to spin precession with *nutation* when a spin polarized electron is injected into the quantum device and is transmitted to the leads. The orientation of transmitted electron spin is shown to be rotated to a certain direction sensitively depending on the details of spin-flip scattering in the quantum device even though the leads are ideal. We discuss spin polarization and nutation in a two-dimensional semiconductor with SO interactions.

In Secs. II and VI, we illustrate spin orientation and polarization in a ballistic semiconductor device. We consider the scattering state in a lead in Sec. II. The particle density matrix for the scattering state will be written in terms of charge-density and spin-density matrix. The orientation of the electron spin is defined as a function of charge-density and spin-density vector. In Sec. III, the orientation vector of the electron spin will be used to show that the spatial spin precession and nutation are due to the spin dependence of electron momentum. Section IV is devoted to spin polarization based on the spin orientation vectors. An ideal lead is considered for spin orientation and polarization in Sec. V. Spatial spin nutation and perfect spin polarization are discussed in a ballistic semiconductor nanostructure with spin-orbit interactions in Sec. VI. Finally, the conclusions are given in Sec. VII.



FIG. 1. (Color online) Quantum device with spin-orbit interactions. When a spin-polarized electron with an arbitrary spin orientation is injected from the one lead to the quantum device, it experiences spin-dependent scattering and is transmitted to the other lead. The transmitted and reflected electron spins have a different orientation from the orientation of injected electron spin due to the spin-dependent scattering even though the leads are ideal. This is discussed in detail in Sec. V. In the region of the quantum device, the SO interaction causes the change of the orientation of electron spin in position. In Secs. III and IV, this can be understood in terms of spatial spin precession and nutation, as shown in Figs. 2 and 3. In Sec. VI, both spin precession and nutation are shown to play an important role for spin-polarized transmissions in ballistic semiconductor heterostructures.

II. SPIN DENSITY MATRIX AND SPIN ORIENTATION VECTOR

Let us start with the scattering state $|\Psi(\mathbf{r})\rangle$ in a lead attached to a quantum device, where $\mathbf{r} \in L$ with L being the index for leads (see Fig. 1). $|\Psi(\mathbf{r})\rangle$ is a two-component spinor that is given in a superposition of the eigenfunctions obtained from the Hamiltonian H_L . Then, the scattering state is in a pure state. In the lead, the charge-density $q(\mathbf{r})$ and spin-density vector $\mathbf{s}(\mathbf{r})$ are given by

$$q(\mathbf{r}) = \langle \Psi(\mathbf{r}') | e \delta(\mathbf{r} - \mathbf{r}') | \Psi(\mathbf{r}') \rangle, \quad (1a)$$

$$\mathbf{s}(\mathbf{r}) = \frac{\hbar}{2} \langle \Psi(\mathbf{r}') | \boldsymbol{\sigma} \delta(\mathbf{r} - \mathbf{r}') | \Psi(\mathbf{r}') \rangle, \quad (1b)$$

where $\boldsymbol{\sigma}$ is the vector of the Pauli matrices.

From the scattering state, one can introduce the (two by two) particle density matrix,

$$\rho(\mathbf{r}) = |\Psi(\mathbf{r})\rangle \langle \Psi(\mathbf{r})|. \quad (2)$$

In terms of the charge-density and spin-density vector, we see the particle density matrix,

$$\rho(\mathbf{r}) = \frac{1}{2} \left(\frac{q(\mathbf{r})}{e} 1 + \frac{2}{\hbar} \mathbf{s}(\mathbf{r}) \cdot \boldsymbol{\sigma} \right). \quad (3)$$

To get more insight into the spin orientation (spin polarization) in electron transport through a ballistic quantum nanodevice, one can define the spin-density matrix from the particle density matrix. The particle density matrix is rewritten in a product of the spin-density matrix and the charge density,

$$\rho(\mathbf{r}) = \frac{q(\mathbf{r})}{e} \rho^S(\mathbf{r}), \quad (4)$$

where the spin-density matrix is defined by

$$\rho^S(\mathbf{r}) = \frac{1}{2} (1 + \hat{\mathbf{s}}(\mathbf{r}) \cdot \boldsymbol{\sigma}), \quad (5)$$

with $\text{Tr}[\rho^S(\mathbf{r})] = 1$. It should be noted that $|\hat{\mathbf{s}}(\mathbf{r})| = 1$ since the scattering state is in a pure state. Consequently, $\hat{\mathbf{s}}$ is a unit vector which indicates the direction that electron spin is pointing to. $\hat{\mathbf{s}}$ can be called *spin orientation vector*. The spin orientation vector is determined by $\hat{\mathbf{s}}(\mathbf{r}) = \text{Tr}[\boldsymbol{\sigma} \rho^S(\mathbf{r})]$, i.e.,

$$\hat{\mathbf{s}}(\mathbf{r}) = \frac{2e \mathbf{s}(\mathbf{r})}{\hbar q(\mathbf{r})}. \quad (6)$$

Note that the charge density corresponds to the amplitude of the spin-density vector. Alternatively, it can be shown that $|\mathbf{s}(\mathbf{r})| = (\hbar/2e)q(\mathbf{r})$ from the definition of the spin-density vector. Thus, the spin-density vector of Eqs. (1a) and (1b) is the product of charge-density and the spin orientation vector; that is,

$$\mathbf{s}(\mathbf{r}) = \frac{\hbar}{2e} q(\mathbf{r}) \hat{\mathbf{s}}(\mathbf{r}). \quad (7)$$

This shows that the position dependence of the spin-density vector results from the position dependencies of the charge density and the orientation vector of electron spin. If the charge density is uniform, i.e., $q(\mathbf{r}) = q_0$, the direction of the spin-density vector corresponds directly to that of the spin orientation vector $\hat{\mathbf{s}}(\mathbf{r})$. Note that if the charge density changes in position, the spin-density vector also changes in position even though the spin orientation vector is frozen in a certain direction, $\hat{\mathbf{s}}(\mathbf{r}) = \hat{\mathbf{s}}_0$.

III. SPIN PRECESSION AND NUTATION

To study spin-dependent electron transport through a ballistic quantum device where spin-dependent scatterings occur, normally, an ideal lead attached to the device has been considered. Also, ferromagnetic or paramagnetic (a semiconductor with SO interactions) leads have been paid much attention to propose a spin polarizer/filter.^{21,22} In such leads, the two eigenspinors are a function of eigenmomentum, \mathbf{k}^α ($\alpha = \pm$), since the spin-dependent one-particle interactions make the momentum states of different spin electrons not degenerate. When an electron is injected into the quantum device with a spin eigenmode α , the transmitted scattering state is given in terms of the two spin eigenmodes ($\beta = \pm$) as

$$|\Psi_t^\alpha(\mathbf{r})\rangle = \sum_{\beta=\pm} t_{\beta\alpha} |\phi_{\mathbf{k}}^\beta(\mathbf{r})\rangle, \quad (8)$$

where $|\phi_{\mathbf{k}}^\beta(\mathbf{r})\rangle$'s are the two eigenspinors in the lead. The transmission amplitudes are denoted by $t_{\beta\alpha}$. In fact, the transmission amplitudes correspond to the spin resolved conductances from the Landauer-Büttiker conductance formula, $G_{\alpha\beta} = G_0 |t_{\alpha\beta}|^2$ with the unit conductance $G_0 = e^2/h$.

For the transmitted scattering state, the charge-density and spin-density vector are given by

$$q^\alpha(\mathbf{r}) = \sum_{\beta\beta'} q_{\beta\beta'}^\alpha(\mathbf{r}) = \sum_{\beta\beta'} e t_{\beta\alpha}^* t_{\beta'\alpha} \langle \phi_{\mathbf{k}}^\beta(\mathbf{r}) | \phi_{\mathbf{k}}^{\beta'}(\mathbf{r}) \rangle, \quad (9a)$$

$$\mathbf{s}^\alpha(\mathbf{r}) = \sum_{\beta\beta'} \mathbf{s}_{\beta\beta'}^\alpha(\mathbf{r}) = \sum_{\beta\beta'} \frac{\hbar}{2} t_{\beta\alpha}^* t_{\beta'\alpha} \langle \phi_{\mathbf{k}}^\beta(\mathbf{r}) | \boldsymbol{\sigma} | \phi_{\mathbf{k}}^{\beta'}(\mathbf{r}) \rangle. \quad (9b)$$

For ballistic transport, the eigenspinors have a form;

$$|\phi_{\mathbf{k}}^\beta(\mathbf{r})\rangle = |v_t^\beta|^{-1/2} \exp[i\mathbf{k}^\beta \cdot \mathbf{r}] |\chi_{\mathbf{k}}^\beta\rangle, \quad (10)$$

where v_t^β is the velocity, \mathbf{k}^β is the momentum, and $|\chi_{\mathbf{k}}^\beta\rangle$ is a one by two matrix describing the spin state. For $\beta=\beta'$, the direction of $\hat{\mathbf{s}}_{\beta\beta}^\alpha$ is the same as that of the spin orientation vector in the eigenmode β even if a decay of transmission amplitude from the boundary for an evanescent mode ($\text{Im}[\mathbf{k}] \neq 0$) occurs. In the case of an evanescent mode, the terms, $q_{\beta\beta}^\alpha$ and $\mathbf{s}_{\beta\beta}^\alpha$, can be negligible for large distance from the boundary. It will be shown in detail in Sec. VI. In the case of a propagating mode ($\text{Im}[\mathbf{k}]=0$), the $q_{\beta\beta}^\alpha$ and $\mathbf{s}_{\beta\beta}^\alpha$ are in a constant position. They do not contribute directly to the spatial spin precession and charge modulation.

However, for $\beta \neq \beta'$, the interference terms in the charge-density and spin-density vector are given by

$$q_{+-}^\alpha(\mathbf{r}) = e^{\frac{t_{+\alpha}^* t_{-\alpha}}{\sqrt{|v_t^+||v_t^-|}}} e^{-i\Delta\mathbf{k} \cdot \mathbf{r}} \langle \chi_{\mathbf{k}^+}^+ | \chi_{\mathbf{k}^-}^- \rangle, \quad (11a)$$

$$\mathbf{s}_{+-}^\alpha(\mathbf{r}) = \frac{\hbar}{2} \frac{t_{+\alpha}^* t_{-\alpha}}{\sqrt{|v_t^+||v_t^-|}} e^{-i\Delta\mathbf{k} \cdot \mathbf{r}} \langle \chi_{\mathbf{k}^+}^+ | \boldsymbol{\sigma} | \chi_{\mathbf{k}^-}^- \rangle, \quad (11b)$$

where $\Delta\mathbf{k} = \mathbf{k}^{+*} - \mathbf{k}^-$, $q_{+-}^\alpha = q_{+-}^{\alpha*}$, and $\mathbf{s}_{+-}^\alpha = \mathbf{s}_{+-}^{\alpha*}$. These interference terms show the origin of the spatial modulations of the charge-density and spin-density vector exhibiting an oscillatory behavior along the electron propagating trajectory with the same period. If there is no spin splitting, i.e., $\mathbf{k}^+ = \mathbf{k}^-$, the charge-density and spin-density vector do not depend on the position. Then they are uniform in the lead. This means that the spin orientation vector is fixed to a certain direction determined by the transmission amplitudes.

Once electron has the two different eigenmomenta, i.e., $\mathbf{k}^{+*} \neq \mathbf{k}^-$, the spin-density vector indeed depends on the position even if the spinors $|\chi^\beta(\mathbf{k}^\beta)\rangle = |\chi^\beta\rangle$ are not a function of the electron momentum, i.e., $\langle \chi^+ | \chi^- \rangle = 0$, and the charge density is uniform. The reason is that $\langle \chi^+ | \boldsymbol{\sigma} | \chi^- \rangle \neq 0$. As a consequence, when an electron travels forward to a certain direction $\hat{\mathbf{r}}$ in the lead, the orientation of electron spin changes periodically in position around the effective magnetic field. This is called *spatial spin precession* in ballistic electron transport. If one of two eigenmomenta is imaginary, the electron takes two different modes in which one is evanescent (e.g., \mathbf{k}^+) and the other is propagating (e.g., \mathbf{k}^-). Due the decay of the amplitudes caused by the evanescent mode, the charge-density and spin-density vector approach to $q^\alpha(\mathbf{r}) \approx q_{+-}^\alpha$ and $\mathbf{s}^\alpha(\mathbf{r}) \approx \mathbf{s}_{+-}^\alpha$. In this case, eventually, the evanescent mode makes the spin orientation vector frozen in a specific direction $\hat{\mathbf{s}}^-$ of the propagating mode for larger distance from the boundary.

The oscillatory and periodic behaviors of the densities are characterized by the spin precession length (SPL),^{47,48}

$$r_s = \frac{2\pi}{|\Delta\mathbf{k} \cdot \hat{\mathbf{r}}|}. \quad (12)$$

Here, it should be stressed that the SPL does not depend on the injected electron mode α because the spatial modulation of the densities results from the difference of the two eigenmomenta in the lead. Also, note that SPL is inversely proportional to the momentum difference. For SPL, the spin orientation vector completes one period of precession around the effective magnetic field, that is, $\hat{\mathbf{s}}^\alpha(\mathbf{r}) = \hat{\mathbf{s}}^\alpha(\mathbf{r} + \mathbf{r}_s)$ with $|\hat{\mathbf{s}}^\alpha(\mathbf{r})| = 1$. For $|\Delta\mathbf{k}| = |\Delta\mathbf{k}|_{\min} (|\Delta\mathbf{k}|_{\max})$, SPL becomes $r_s = r_s^{\max} (r_s^{\min})$. For the one period of the spin precession, the amplitude (charge density) of the spin-density vector, $\mathbf{s}^\alpha(\mathbf{r})$, is bounded: $q_{\min}^\alpha \leq q^\alpha(\mathbf{r}) \leq q_{\max}^\alpha$, where $q_{\max(\min)}^\alpha = \sum_\beta |t_{\beta\alpha}|^2 / |v_t^\beta| \pm 2|t_{+\alpha}| |t_{-\alpha}| |\langle \chi_{\mathbf{k}^+}^+ | \chi_{\mathbf{k}^-}^- \rangle| / (|v_t^+| |v_t^-|)^{1/2}$. The change density also is a periodic function of \mathbf{r}_s , $q^\alpha(\mathbf{r}) = q^\alpha(\mathbf{r} + \mathbf{r}_s)$.

It should be addressed that if a spin-splitting occurs in the lead, the position dependency of the spin orientation vector gives rise to a difficulty for spin-polarization observations because the spatial dimension of the lead would be crucial to determine the spin orientation. Spin polarization measurements at different positions of the lead may detect different spin polarizations. As a consequence, an ideal lead would be a prerequisite to observe spin polarization because the spin orientation vector is not changed in the ideal lead. It will be shown in detail in the Sec. V.

Spin precession and shifted angles. Equation (11a) and (11b) shows the variation of $\hat{\mathbf{s}}^\alpha(\mathbf{r})$ during spatial spin precession since $\hat{\mathbf{s}}^\alpha(\mathbf{r})$ is a function of \mathbf{r} . To get more understanding of the spin dynamics from the spin orientation vector, one can introduce two characteristic angles.

*Spin precession angle (SPA)*¹⁴ between the effective magnetic field and the orientation vector of the traveling spin can be defined by

$$\Theta_B^\alpha(\mathbf{r}) = \cos^{-1}[\alpha \hat{\mathbf{B}}_{\text{eff}}(\mathbf{k}_0) \cdot \hat{\mathbf{s}}^\alpha(\mathbf{r})], \quad (13)$$

where \mathbf{k}_0 is the momentum of the incident electron. For $\Theta_B^\alpha(\mathbf{r}) = \Theta_0$ (a constant angle), the electron spin undergoes a gentle spatial spin precession. For $\Theta_B^\alpha(\mathbf{r}) \neq \Theta_0$, on spatial precessing, the electron spin wobbles periodically within $\Theta_B^{\alpha,\min} \leq \Theta_B^\alpha(\mathbf{r}) \leq \Theta_B^{\alpha,\max}$. This wobble of electron spin can be called *spatial spin nutation*. When $\Theta_B^\alpha(\mathbf{r}) = \Theta_B^\alpha(\mathbf{r} + \mathbf{r}_n)$, one can define *spin nutation length* by \mathbf{r}_n . In general, the periods of spin precession and nutation can differ from each other, $\mathbf{r}_s \neq \mathbf{r}_n$. In our case, the nutation has the period of the electron-spin precession, i.e., $\mathbf{r}_s = \mathbf{r}_n$, since $\hat{\mathbf{B}}_{\text{eff}}(\mathbf{k}_0)$ is constant and $\hat{\mathbf{s}}^\alpha(\mathbf{r}) = \hat{\mathbf{s}}^\alpha(\mathbf{r} + \mathbf{r}_s)$. This nutation is caused by the interference of two spin modes. Figure 2 shows the pictorial explanation for the spin precession and nutation.

The orientation of the incident spin changes during the spin-dependent scattering. Then, the difference between the orientations of the incident and transmitted spins is defined as *spin shifted angle (SA)*,

$$\Theta_{\text{SA}}^\alpha(\mathbf{r}) = \cos^{-1}[\hat{\mathbf{s}}_0 \cdot \hat{\mathbf{s}}^\alpha(\mathbf{r})], \quad (14)$$

where $\hat{\mathbf{s}}_0$ and $\hat{\mathbf{s}}^\alpha$ are the orientations of incident spin and transmitted spins, respectively. For instance, if $\hat{\mathbf{s}}^\alpha \parallel \hat{\mathbf{s}}_0$ ($\hat{\mathbf{s}}^\alpha \perp \hat{\mathbf{s}}_0$) then $\Theta_{\text{SA}}^\alpha = 0$ or π ($\Theta_{\text{SA}}^\alpha = \pi/2$).

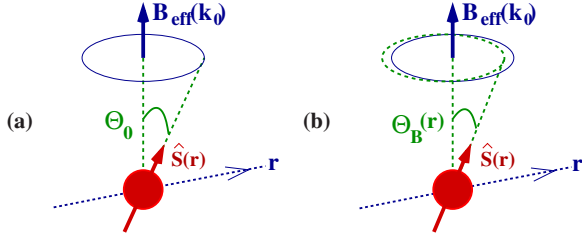


FIG. 2. (Color online) Schematic illustration of spatial spin precession and nutation in the presence of spin-orbit interactions. When a spin-polarized electron with the momentum \mathbf{k}_0 is injected into the region with SO interactions, the transmitted electron spin in the region feels the effective magnetic field $\mathbf{B}_{\text{eff}}(\mathbf{k})$, resulting from the SO interactions, which changes in direction. Here, $\hat{\mathbf{s}}^\alpha(\mathbf{r})$ is the spin orientation vector for the injection mode α and $|\hat{\mathbf{s}}^\alpha(\mathbf{r})|=1$. $\Theta(\mathbf{r})$ denotes the angle between $\mathbf{B}_{\text{eff}}(\mathbf{k}_0)$ and $\hat{\mathbf{s}}^\alpha(\mathbf{r})$. (a) $\Theta_B(\mathbf{r})=\Theta_0$. If the angle between the effective magnetic field and the spin orientation vector $\hat{\mathbf{s}}(\mathbf{r})$ of the traveling electron spin is constant, the electron spin precesses around the direction of $\mathbf{B}_{\text{eff}}(\mathbf{k}_0)$ along the trajectory (dashed arrow) which the electron spin takes. For ballistic transport, the period of the spatial precession is given by the spin precession length $r_s=2\pi/|\Delta\mathbf{k}\cdot\hat{\mathbf{r}}|$. $\Delta\mathbf{k}$ is the difference of two eigenmomenta. (b) $\Theta_B^{\min}\leq\Theta_B(\mathbf{r})\leq\Theta_B^{\max}$. Generally, $\hat{\mathbf{B}}_{\text{eff}}(\mathbf{k}_0)\cdot\hat{\mathbf{s}}^\alpha(\mathbf{r})\neq\text{const}$. Since the spin orientation vector $\hat{\mathbf{s}}(\mathbf{r})$ is a periodic function of \mathbf{r} , the angle has a value in between its maximum and minimum. This implies that the orientation of electron spin wobbles on the spin precession, which can be called *spatial spin nutation*.

IV. SPIN POLARIZATION

So far, we have discussed the orientation of transmitted spins for spin-polarized injection. In the present section, we investigate spin polarization when the injected electron is not spin polarized. We consider the total particle density matrix as the sum of the particle density matrices with the injected spin eigenmodes ($\alpha=\pm$);

$$\rho^T(\mathbf{r})=\rho^+(\mathbf{r})+\rho^-(\mathbf{r})=\frac{q_T(\mathbf{r})}{e}\rho_T^S(\mathbf{r}), \quad (15)$$

where the total charge density is $q_T(\mathbf{r})=q^+(\mathbf{r})+q^-(\mathbf{r})$. The total spin-density matrix has a form:

$$\rho_T^S(\mathbf{r})=\frac{1}{2}(1+\mathbf{P}(\mathbf{r})\cdot\boldsymbol{\sigma}). \quad (16)$$

The spin-polarization vector $\mathbf{P}(\mathbf{r})$ at position \mathbf{r} is given in terms of the spin orientation vectors $\hat{\mathbf{s}}^\alpha$ as follows:

$$\mathbf{P}(\mathbf{r})=\frac{q^+(\mathbf{r})}{q_T(\mathbf{r})}\hat{\mathbf{s}}^+(\mathbf{r})+\frac{q^-(\mathbf{r})}{q_T(\mathbf{r})}\hat{\mathbf{s}}^-(\mathbf{r}). \quad (17)$$

Let us rewrite the spin-polarization vector in a form $\mathbf{P}(\mathbf{r})=P(\mathbf{r})\hat{\mathbf{p}}(\mathbf{r})$, where its amplitude is

$$P(\mathbf{r})=\left\{1-2\frac{q^+(\mathbf{r})q^-(\mathbf{r})}{q_T^2(\mathbf{r})}[1-\hat{\mathbf{s}}^+(\mathbf{r})\cdot\hat{\mathbf{s}}^-(\mathbf{r})]\right\}^{1/2}, \quad (18)$$

with its direction,

$$\hat{\mathbf{p}}(\mathbf{r})=\frac{q^+(\mathbf{r})\hat{\mathbf{s}}^+(\mathbf{r})+q^-(\mathbf{r})\hat{\mathbf{s}}^-(\mathbf{r})}{\{q_T^2(\mathbf{r})-2q^+(\mathbf{r})q^-(\mathbf{r})[1-\hat{\mathbf{s}}^+(\mathbf{r})\cdot\hat{\mathbf{s}}^-(\mathbf{r})]\}^{1/2}}. \quad (19)$$

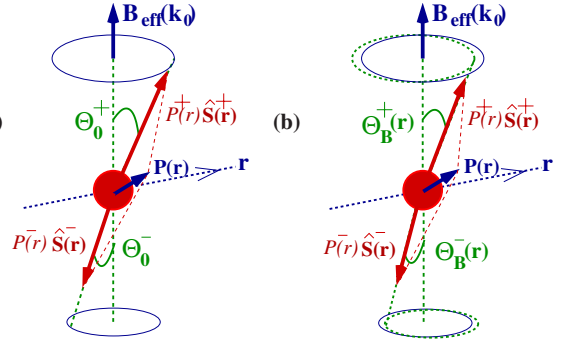


FIG. 3. (Color online) Schematic illustration of spin-polarization vectors for a lead with spin-orbit interaction. When a spin-unpolarized electron with the spin eigenmodes ($\alpha=\pm$) and the momentum \mathbf{k}_0 is injected into the region with SO interactions, the electron spin in the SO interacting region feels the effective magnetic field, $\alpha\mathbf{B}_{\text{eff}}(\mathbf{k})$. The spin-polarization vector is given by $\mathbf{P}(\mathbf{r})=\sum_\alpha P^\alpha(\mathbf{r})\hat{\mathbf{s}}^\alpha(\mathbf{r})$, where $P^\alpha(\mathbf{r})=q^\alpha(\mathbf{r})/[q^+(\mathbf{r})+q^-(\mathbf{r})]$. Here, $\hat{\mathbf{s}}^\alpha(\mathbf{r})$ is the spin orientation vector. α indicates the injection mode and $|\hat{\mathbf{s}}^\alpha(\mathbf{r})|=1$. $\Theta^\alpha(\mathbf{r})$ denotes the angle between $\mathbf{B}_{\text{eff}}(\mathbf{k}_0)$ and $\hat{\mathbf{s}}^\alpha(\mathbf{r})$. The period of the spin polarization is the spin precession length, $r_s=2\pi/|\Delta\mathbf{k}\cdot\hat{\mathbf{r}}|$. The spin-polarization vectors are shown pictorially (a) in the case of spin precession with no nutation, $\Theta_B^\alpha(\mathbf{r})=\Theta_0^\alpha$, and (b) in the case of spin precession with nutation, $\Theta_B^{\alpha,\min}\leq\Theta_B^\alpha(\mathbf{r})\leq\Theta_B^{\alpha,\max}$.

The spin polarization is bounded: $0\leq P\leq 1$. When $\hat{\mathbf{s}}^+\cdot\hat{\mathbf{s}}^-=1$ ($\hat{\mathbf{s}}^+\parallel\hat{\mathbf{s}}^-$) i.e., $\hat{\mathbf{s}}^+=\hat{\mathbf{s}}^-$, the electron spin is fully polarized, $P=1$ and $\hat{\mathbf{p}}=\hat{\mathbf{s}}^+$. The full spin polarization can be archived in the presence of an evanescent mode. It will be discussed in a ballistic semiconductor nanostructures in Sec. VI. For $\hat{\mathbf{s}}^+\cdot\hat{\mathbf{s}}^-=-(q^-/q^+-q^+/q^-)/2$, electron spin is not polarized, $P=0$. For $0<P<1$, electron spin is partially polarized. The examples include (i) for $\hat{\mathbf{s}}^+\cdot\hat{\mathbf{s}}^-=1$ ($\hat{\mathbf{s}}^+\parallel\hat{\mathbf{s}}^-$), i.e., $\hat{\mathbf{s}}^+=\hat{\mathbf{s}}^-$, $P=(q^+-q^-)/(q^++q^-)$ and $\hat{\mathbf{p}}=\hat{\mathbf{s}}^+$, and (ii) for $\hat{\mathbf{s}}^+\cdot\hat{\mathbf{s}}^-=0$ ($\hat{\mathbf{s}}^+\perp\hat{\mathbf{s}}^-$), $P=\sqrt{1-2q^+q^-/q_T^2}$ and $\hat{\mathbf{p}}=(q^+\hat{\mathbf{s}}^++q^-\hat{\mathbf{s}}^-)/(q^++q^-)^{1/2}$.

A pictorial explanation of spin precession and nutation for spin polarization is displayed in Fig. 3. If SPAs are constants, i.e., $\hat{\mathbf{s}}^\alpha(\mathbf{r})=\hat{\mathbf{s}}_0^\alpha$, $P(\mathbf{r})$ does not depend on the spin nutation. Then, the spin polarization can be observed via the spin-dependent charge modulations. In addition, the spin polarization is oscillating with the period of the SPL because $r_s=r_n$. However, Eq. (18) clearly shows that spin nutation plays an important role in determining the spin polarization because of the term $\hat{\mathbf{s}}^+(\mathbf{r})\cdot\hat{\mathbf{s}}^-(\mathbf{r})$. Therefore, for spin splitting in the lead, the spin polarization can not be measured only by the spin-dependent charge modulations.

Similarly, the spin orientations and polarizations of reflected spin in the injected lead and traveling spins through the quantum device can be determined by the spin-density matrices for reflected spin in the injection lead and for traveling spin inside the quantum device, respectively.

V. IDEAL LEADS

No spin splitting of bands occurs in ideal leads. Electrons with different spins have the same momentum $\mathbf{k}^+=\mathbf{k}^-=\mathbf{k}$ ($v^+=v^-=v_F$). The spinors do not depend on the momentum,

i.e., $\langle \chi^\beta | \chi^{\beta'} \rangle = \beta \delta_{\beta\beta'}$. From Eqs. (9a) and (9b), the spin orientation vectors of transmitted electron are given by

$$\hat{\mathbf{s}}^\alpha = 2 \operatorname{Re} \left[\frac{t_{+\alpha}^* t_{-\alpha} \mathbf{n}_p}{|t_{+\alpha}|^2 + |t_{-\alpha}|^2} \right] + \frac{|t_{+\alpha}|^2 - |t_{-\alpha}|^2}{|t_{+\alpha}|^2 + |t_{-\alpha}|^2} \mathbf{n}_+, \quad (20)$$

where $\mathbf{n}_\alpha = \langle \chi^\alpha | \boldsymbol{\sigma} | \chi^\alpha \rangle$ and $\mathbf{n}_p = \langle \chi^+ | \boldsymbol{\sigma} | \chi^- \rangle$. Here, $\mathbf{n}_+ = -\mathbf{n}_-$ and $\mathbf{n}_\alpha \perp \mathbf{n}_p$. Hence, the spin orientation vectors are determined only by the transmission amplitudes $t_{\alpha\beta}$. If one choose the spin states of the ideal lead as

$$|\chi^+\rangle = \begin{pmatrix} 1 \\ 0 \end{pmatrix}, \text{ and } |\chi^-\rangle = \begin{pmatrix} 0 \\ 1 \end{pmatrix}$$

the unit direction vectors are given by $\mathbf{n}_\alpha = \alpha \hat{\mathbf{z}}$ and $\mathbf{n}_p = \hat{\mathbf{x}} - i\hat{\mathbf{y}}$. As expected, $|\hat{\mathbf{s}}_\alpha| = 1$ and the spin orientation of a transmitted electron in ideal leads is frozen in a certain direction containing characteristics of spin-dependent scattering in the quantum device.

If the spin orientation of injected electron is $\hat{\mathbf{s}}_0 = \mathbf{n}_+$, the shifted angle between the injected and transmitted spin is given by

$$\Theta_{\text{SA}}^\alpha = \cos^{-1} \left[\frac{|t_{+\alpha}|^2 - |t_{-\alpha}|^2}{|t_{+\alpha}|^2 + |t_{-\alpha}|^2} \right]. \quad (21)$$

This shows that the angle deviation from the orientation of injected spin is a function of the transmission amplitudes $t_{\pm\alpha}$. Obviously, the transmission amplitudes can be varied by the controllable parameters of the quantum devices. (i) For strong spin-flip scattering, $|t_{++}| \ll |t_{-+}|$ ($|t_{--}| \ll |t_{+-}|$), the transmitted spin has the opposite orientation of the injected spin, that is, $\Theta_{\text{SA}}^+ \approx \pi$. Thus, for the strong spin-flip scattering, the spin orientation vector of the transmitted spin is $\hat{\mathbf{s}}^\alpha \approx -\mathbf{n}_\alpha = -\alpha \hat{\mathbf{z}}$. It implies that the injected spin undergoes spin flipping during scattering in the quantum device. (ii) Whereas, for the weak spin-flip scattering in the quantum device, $|t_{++}| \gg |t_{-+}|$ and $|t_{--}| \gg |t_{+-}|$, the spin orientation vector is not changed as $\hat{\mathbf{s}}^\alpha \approx \mathbf{n}_\alpha = \alpha \hat{\mathbf{z}}$. The SA becomes $\Theta_{\text{SA}}^+ \approx 0$. (iii) For the intermediate spin-flip scattering, i.e., $|t_{+\alpha}| \approx |t_{-\alpha}|$ and $t_{\alpha\beta}$ are real, the spin orientation vector becomes $\hat{\mathbf{s}}^\alpha \approx \alpha \hat{\mathbf{x}}$ and $\Theta^\alpha \approx \alpha\pi/2$.

When the injected electron is not spin-polarized, the spin-polarization vector is written in terms of the transmission amplitudes;

$$\mathbf{P} = \operatorname{Re}[P_\perp \mathbf{n}_p] + P_\parallel \mathbf{n}_+, \quad (22a)$$

where P_\parallel and P_\perp are given by

$$P_\parallel \equiv \frac{|t_{++}|^2 + |t_{+-}|^2 - |t_{-+}|^2 - |t_{--}|^2}{|t_{++}|^2 + |t_{+-}|^2 + |t_{-+}|^2 + |t_{--}|^2}, \quad (22b)$$

$$P_\perp \equiv \frac{2(t_{++}^* t_{-+} + t_{+-}^* t_{--})}{|t_{++}|^2 + |t_{+-}|^2 + |t_{-+}|^2 + |t_{--}|^2}. \quad (22c)$$

This equation was found in Ref. 18 for an ideal lead. If there is no spin-dependent scattering in the quantum device, the spin channels are decoupled and not mixed, i.e., $t_{+-} = t_{-+} = 0$. Since the injected electron is not spin-polarized, i.e., $|t_{++}| = |t_{--}|$, the transmitted electron is not spin-polarized, $\mathbf{P} = 0$ ($P_\parallel = 0$ and $P_\perp = 0$). However, if spin-dependent scattering oc-

curs in the quantum device, the spin channels are mixed and spin-flipped electrons can propagate out to the ideal lead. For the weak spin-flip scattering, $\mathbf{P} \approx P \hat{\mathbf{z}}$ because $\hat{\mathbf{s}}^\alpha \approx \alpha \hat{\mathbf{z}}$ and, for the strong spin-flip scattering, $\mathbf{P} \approx -P \hat{\mathbf{z}}$ because $\hat{\mathbf{s}}^\alpha \approx -\alpha \hat{\mathbf{z}}$. Here, $P = (q^+ - q^-)/(q^+ + q^-)$. In the intermediate regime of $|t_{+\alpha}| \approx |t_{-\alpha}|$ ($t_{\alpha\beta}$ are real), $\mathbf{P} \approx P \hat{\mathbf{x}}$ because $\hat{\mathbf{s}}^\alpha \approx \alpha \hat{\mathbf{x}}$. Hence, it should be noted that the direction of the spin-polarization vector is sensitive to spin-flip scattering in the quantum device.

VI. BALLISTIC SEMICONDUCTOR NANOSTRUCTURES WITH SPIN-ORBIT INTERACTIONS

In this section, the effects of spatial spin nutation will be investigated explicitly in two-dimensional semiconductor junctions with SO interactions. Let us consider the lateral interface ($x=0$) dividing the two-dimensional semiconductor (xz -plane) into two regions with different strengths of SO interactions.²¹ Here, we consider the Rashba SO interaction, $H_{\text{SO}} = a \mathbf{B}_{\text{eff}} \cdot \boldsymbol{\sigma}$ with a being the strength of the SO interaction, where $\mathbf{B}_{\text{eff}}(\mathbf{k}) = k_z \hat{\mathbf{x}} - k_x \hat{\mathbf{z}} = k \sin \phi \hat{\mathbf{x}} - k \cos \phi \hat{\mathbf{z}}$. When an electron in a spin eigenmode ($\alpha = \pm$) is injected into the interface from the one region ($x < 0$), the scattering state for the other region ($x > 0$) has the form of Eq. (8) in terms of the two spin eigenmodes ($\beta = \pm$). For the scattering state, the two spinors are given by

$$|\chi_{\mathbf{k}}^+\rangle = A_+^{-1/2} \begin{pmatrix} \sin \frac{\phi_+}{2} \\ \cos \frac{\phi_+}{2} \end{pmatrix}, \quad |\chi_{\mathbf{k}}^-\rangle = A_-^{-1/2} \begin{pmatrix} \cos \frac{\phi_-}{2} \\ -\sin \frac{\phi_-}{2} \end{pmatrix}, \quad (23)$$

where $A_\alpha = \cosh \phi_\alpha^I$ with $\phi_\alpha^I = \operatorname{Im}[\phi_\alpha]$ and $\phi_\alpha^R = \operatorname{Re}[\phi_\alpha]$. The angle variables ϕ_α are a function of the electron momentum and the SO interaction strengths. Once the injection angle ϕ_0 of the incident electron is fixed, the angle variables are determined by the wave vector conservation at the interface. Since the wave function should be continuous across the interface ($x=0$), the imposed conservation of the wave number is $k_z = k_z^+ = k_z^-$ or $k_F \sin \phi_0 = k_F^+ \sin \phi_+ = k_F^- \sin \phi_-$. Then, the angle variables for the two different modes differ from each other, $\phi_+ \neq \phi_-$. Here, k_F is the momentum of the incident electron and $k_F^\alpha = -\alpha k_a + \sqrt{k_a^2 + \varepsilon}$ with $k_a = m^* a / \hbar^2$ and $\varepsilon = 2m^* E / \hbar$. This implies that, in general, (i) the electron spins for the two eigenmodes are not collinear and (ii) the transmitted electron through the interface takes two different trajectories.

Spatial spin precession and nutation. Let us first consider the case of spin-polarized injection. From Eqs. (9a) and (9b), the spin orientation vectors of the transmitted electron are given by

$$\hat{\mathbf{s}}^\alpha(\mathbf{r}) = \frac{\operatorname{Re}[2B_1^\alpha(\mathbf{r})\mathbf{n}_p] + \sum_\beta B_{2\beta}^\alpha(\mathbf{r})\mathbf{n}_\beta}{\operatorname{Re}[2B_1^\alpha(\mathbf{r})\sin \varphi_-] + \sum_\beta B_{2\beta}^\alpha(\mathbf{r})}, \quad (24)$$

where

$$\mathbf{n}_p = A_+^{-1} A_-^{-1} (\cos \varphi_+ \hat{\mathbf{x}} + i \cos \varphi_- \hat{\mathbf{y}} + \sin \varphi_+ \hat{\mathbf{z}}),$$

$$\mathbf{n}_\alpha = \alpha A_\alpha^{-1} (\sin \phi_\alpha^R \hat{\mathbf{x}} - \alpha \sinh \phi_\alpha^I \hat{\mathbf{y}} + \cos \phi_\alpha^R \hat{\mathbf{z}}),$$

$$B_1^\alpha(\mathbf{r}) = |t_{+\alpha}| |t_{-\alpha}| e^{-i(\theta_\alpha + \Delta \mathbf{k} \cdot \mathbf{r})} / (|v_t^+| |v_t^-|)^{1/2},$$

and $B_{2\beta}^\alpha(\mathbf{r}) = |t_{\beta\alpha}|^2 e^{-2 \text{Im} \mathbf{k}^\beta \cdot \mathbf{r}} / |v_t^\beta|$ with $\varphi_\pm = (\phi_\pm^* \pm \phi_-)/2$ and $\theta_\alpha = \arg[t_{+\alpha}] - \arg[t_{-\alpha}]$. One can find that the $\hat{\mathbf{s}}^\alpha$ satisfy $|\hat{\mathbf{s}}^\alpha| = 1$. The SPL is given by $r_s = 2\pi |k_F^+ \cos \phi_+^* - k_F^- \cos \phi_-| \hat{\mathbf{x}} \cdot \hat{\mathbf{r}}^{-1}$, since $\mathbf{k}^\beta = (k_x^\beta, 0, k_z^\beta)$ and $\mathbf{r} = (x, 0, z)$.

If $k_F > k_F^\alpha$, total internal reflections²¹ occurs because the channel α becomes an evanescent mode. The critical angle ϕ_c can be defined from $k_F = k_F^\alpha$. For $\phi_0 > \phi_c$, ϕ_α becomes complex. If $k_F < k_F^\alpha$, no evanescent mode exists, that is, ϕ_+ and ϕ_- are real. For $\phi_0 < \phi_c$ and $\varphi_- \ll 1$, $\phi^{*+} \approx \phi_-$ (i.e., $\varphi_+ \sim \phi_0$ and $\varphi_- \sim 0$). The spin precession angle becomes

$$\Theta_B^\alpha(\mathbf{r}) \approx \cos^{-1} \left[\frac{\text{Re}[B_1^\alpha] \sin 2\phi_0 - (B_{2+}^\alpha - B_{2-}^\alpha) \cos 2\phi_0}{\sum_\beta B_{2\beta}^\alpha} \right]. \quad (25)$$

Note that only B_1^α is a function of \mathbf{r} . It means that the nutation has the same period as the precession. For the normal incidence $\phi_0 = 0$, the direction of the effective magnetic field is $\hat{\mathbf{B}}_{\text{eff}} = -\hat{\mathbf{z}}$ and the transmitted angles are $\phi_+^* = \phi_- = 0$. Since $\Theta_B^\alpha(\mathbf{r}) = \cos^{-1} [(|t_{+\alpha}|^2 |v_t^-| - |t_{-\alpha}|^2 |v_t^+|) / (|t_{+\alpha}|^2 |v_t^-| + |t_{-\alpha}|^2 |v_t^+|)]$ for the normal incidence, the transmitted electron propagates with simple spin precession (*no nutation*) around $\hat{\mathbf{B}}_{\text{eff}} = -\hat{\mathbf{z}}$ [see Fig. 2(a)]. The period of the spin precession is $r_s = \pi/k_\alpha$, where $|\Delta \mathbf{k}| = |\Delta \mathbf{k}|_{\text{min}} = 2k_\alpha$, for the normal transmission.¹³

As the incident angle increases, $\Theta_B^\alpha(\mathbf{r})$ is not constant anymore. Then, the transmitted spin undergoes a precession *with nutation* around $\hat{\mathbf{B}}_{\text{eff}} = \sin \phi_0 \hat{\mathbf{x}} - \cos \phi_0 \hat{\mathbf{z}}$ [see Fig. 2(b)]. As an example, for $\phi_0 = \pi/4$, $\hat{\mathbf{B}}_{\text{eff}} = (\hat{\mathbf{x}} - \hat{\mathbf{z}}) / \sqrt{2}$ and $\Theta_B^\alpha(\mathbf{r}) \approx \cos^{-1} [\text{Re}[B_1^\alpha] / \sum_\beta B_{2\beta}^\alpha]$. At $\phi_0 = \phi_c$, $r_s = r_s^{\text{max}}$ because the momentum difference becomes $|\Delta \mathbf{k}| = |\Delta \mathbf{k}|_{\text{max}}$. For an incident angle larger than the critical angle $\phi_0 > \phi_c$, i.e., for the total internal reflection, an interference between the propagating mode \mathbf{k}^- and the evanescent mode ($\mathbf{k}^+ = \text{Im}[\mathbf{k}^+] > 0$) occurs. In this case, for $r_s \ll r$, due to the decay $e^{-\text{Im}[\mathbf{k}^+] \cdot \mathbf{r}}$, B_1^α and B_{2+}^α reaches zero exponentially. Interestingly, in the limit of $r_s \ll r$, the orientation of electron spin $\hat{\mathbf{s}}^\alpha(\mathbf{r})$ approaches to $\mathbf{n}_- = -\sin \phi_- \hat{\mathbf{x}} + \cos \phi_- \hat{\mathbf{z}}$ regardless of the orientations of the incident spins.

Spin polarization. Next, let us discuss the case in which the injected electron is not spin polarized. From Eq. (17), the spin-polarization vector is given by

$$\mathbf{P}(\mathbf{r}) = \frac{\text{Re} \left[\sum_\alpha 2B_1^\alpha(\mathbf{r}) \mathbf{n}_p \right] + \sum_{\alpha, \beta} B_{2\beta}^\alpha \mathbf{n}_\beta}{\sum_\alpha \left(\text{Re}[2B_1^\alpha(\mathbf{r}) \sin \varphi_-] + \sum_\beta B_{2\beta}^\alpha \right)}. \quad (26)$$

Note that the function B_1^α depends on \mathbf{r} . Then, the spin polarization depends on the position \mathbf{r} . This position dependency of the spin polarization might be one of difficulties of the spin-polarization measurement.

For the normal incidence $\phi_0 = 0$, the spin-polarization vector becomes

$$\mathbf{P}(\mathbf{r}) = \frac{\text{Re} \left[\sum_\alpha 2B_1^\alpha(\mathbf{r}) (\hat{\mathbf{x}} + i\hat{\mathbf{y}}) \right]}{\sum_{\alpha\beta} B_{2\beta}^\alpha} + \frac{(B_{2+}^\alpha - B_{2-}^\alpha) \hat{\mathbf{z}}}{\sum_{\alpha\beta} B_{2\beta}^\alpha}. \quad (27)$$

Note that the z component of the spin-polarization vector is constant. This implies that the spin-polarization vector rotates around the spin quantized axis of $\hat{\mathbf{z}}$ with a constant angle. In this case, the charge density is uniform, i.e., $q^T = \sum_{\alpha\beta} B_{2\beta}^\alpha$, but the amplitude of the spin-polarization vector is a periodic function of \mathbf{r} due to the spin precession.

As the incident angle increases, the spin nutation plays a crucial role in determining the spin polarization. That is, for $\phi_0 < \phi_c$ and $\varphi_- \ll 1$, $\phi^{*+} \approx \phi_-$ (i.e., $\varphi_+ \sim \phi_0$ and $\varphi_- \sim 0$). The projection of the spin-polarization vector onto the spin quantized axis of $\hat{\mathbf{z}}$ is given by

$$P_z = \frac{\text{Re} \left[\sum_\alpha 2B_1^\alpha(\mathbf{r}) \right]}{\sum_{\alpha\beta} B_{2\beta}^\alpha} \sin \phi_0 + \frac{(B_{2+}^\alpha - B_{2-}^\alpha)}{\sum_{\alpha\beta} B_{2\beta}^\alpha} \cos \phi_0. \quad (28)$$

Compared to the z component of Eq. (27), it is clear that the additional term in the z component of the spin-polarization vector is a function of the position \mathbf{r} due to the spin nutation. For $\phi_0 > \phi_c$, the decay, $e^{-\text{Im}[\mathbf{k}^+] \cdot \mathbf{r}}$, of the evanescent mode makes B_1^α and B_{2+}^α reaches zero exponentially as r increases. Then, in the limit of $r_s \ll r$, the electron spin is fully polarized; $\mathbf{P}(\mathbf{r}) \approx -\sin \phi_- \hat{\mathbf{x}} + \cos \phi_- \hat{\mathbf{z}}$. In other words, at large distance from the interface, electron has just one spin channel for propagating. Therefore, this property can be used to develop a spin filter and/or polarizer in ballistic semiconductor devices.²¹

VII. CONCLUSIONS

We investigated spin orientation and polarization in ballistic semiconductor nanostructures. A particle density matrix is employed in order to determine the orientation and polarization of electron spin. The amplitude of the spin-density vector is shown to correspond to the charge density that can be observed in experiments by charge modulation measurement. It is found that the quantum interference between two spin eigenmodes induces *spatial spin nutation* in electron transport. The spin polarization has been shown to strongly

depend on the spin nutation. In ballistic semiconductor junctions, an evanescent spin-dependent channel is shown to enable a realization of full spin polarization when the system size r is much larger than the spatial spin precession length r_s . Such a full spin polarization makes it possible to design a spin filtering/polarizing electronic device.

ACKNOWLEDGMENTS

We thank Ross H. McKenzie and Ulrich Zülicke for inspiring this work. We acknowledge the support from the National Science Foundation Project of CQ CSTC and the Australian Research Council.

*sycho@cqu.edu.cn

- ¹D. D. Awschalom and J. M. Kikkawa, *Phys. Today* **52**(6), 33 (1999).
- ²S. A. Wolf, D. D. Awschalom, R. A. Buhrman, J. M. Daughton, S. von Molnár, M. L. Roukes, A. Y. Chtchelkanova, and D. M. Treger, *Science* **294**, 1488 (2001).
- ³*Semiconductor Spintronics and Quantum Computation*, edited by D. D. Awschalom, D. Loss, and N. Samarth (Springer-Verlag, Berlin, 2002).
- ⁴I. Žutić, J. Fabian, and S. Das Sarma, *Rev. Mod. Phys.* **76**, 323 (2004).
- ⁵Y. Meir, Y. Gefen, and O. Entin-Wohlman, *Phys. Rev. Lett.* **63**, 798 (1989).
- ⁶T. Choi, S. Y. Cho, C.-M. Ryu, and C. K. Kim, *Phys. Rev. B* **56**, 4825 (1997).
- ⁷T.-Z. Qian and Z.-B. Su, *Phys. Rev. Lett.* **72**, 2311 (1994).
- ⁸M. König, A. Tschetschetkin, E. M. Hankiewicz, J. Sinova, V. Hock, V. Daumer, M. Schäfer, C. R. Becker, H. Buhmann, and L. W. Molenkamp, *Phys. Rev. Lett.* **96**, 076804 (2006).
- ⁹A. G. Aronov and Y. B. Lyanda-Geller, *Phys. Rev. Lett.* **70**, 343 (1993).
- ¹⁰A. F. Morpurgo, J. P. Heida, T. M. Klapwijk, B. J. van Wees, and G. Borghs, *Phys. Rev. Lett.* **80**, 1050 (1998).
- ¹¹D. Frustaglia, M. Hentschel, and K. Richter, *Phys. Rev. Lett.* **87**, 256602 (2001).
- ¹²Y. Lyanda-Geller, *Phys. Rev. Lett.* **71**, 657 (1993).
- ¹³S. Datta and B. Das, *Appl. Phys. Lett.* **56**, 665 (1990).
- ¹⁴R. Winkler, *Phys. Rev. B* **69**, 045317 (2004).
- ¹⁵M. Lee and M.-S. Choi, *Phys. Rev. B* **71**, 153306 (2005).
- ¹⁶M.-H. Liu, C.-R. Chang, and S.-H. Chen, *Phys. Rev. B* **71**, 153305 (2005).
- ¹⁷M. G. Pala, M. Governale, J. König, U. Zülicke, and G. Iannaccone, *Phys. Rev. B* **69**, 045304 (2004).
- ¹⁸B. K. Nikolić and S. Souma, *Phys. Rev. B* **71**, 195328 (2005).
- ¹⁹H.-Q. Zhou and S. Y. Cho, *J. Phys.: Condens. Matter* **17**, 7433 (2005).
- ²⁰J. Nitta, T. Akazaki, H. Takayanagi, and T. Enoki, *Phys. Rev. Lett.* **78**, 1335 (1997).
- ²¹M. Khodas, A. Shekhter, and A. M. Finkel'stein, *Phys. Rev. Lett.* **92**, 086602 (2004).
- ²²P. Šeba, P. Exner, K. N. Pichugin, A. Vyhnal, and P. Středa, *Phys. Rev. Lett.* **86**, 1598 (2001).
- ²³J. Splettstoesser, M. Governale, and U. Zülicke, *Phys. Rev. B* **68**, 165341 (2003).
- ²⁴A. I. Signal and U. Zülicke, *Appl. Phys. Lett.* **87**, 102102 (2005).
- ²⁵U. Zülicke, *Appl. Phys. Lett.* **85**, 2616 (2004).
- ²⁶L. P. Rokhinson, V. Larkina, Y. B. Lyanda-Geller, L. N. Pfeiffer, and K. W. West, *Phys. Rev. Lett.* **93**, 146601 (2004).
- ²⁷J. Sinova, D. Culcer, Q. Niu, N. A. Sinitsyn, T. Jungwirth, and A. H. MacDonald, *Phys. Rev. Lett.* **92**, 126603 (2004).
- ²⁸E. G. Mishchenko, A. V. Shytov, and B. I. Halperin, *Phys. Rev. Lett.* **93**, 226602 (2004).
- ²⁹V. Sih, W. H. Lau, R. C. Myers, V. R. Horowitz, A. C. Gossard, and D. D. Awschalom, *Phys. Rev. Lett.* **97**, 096605 (2006).
- ³⁰B. K. Nikolić, S. Souma, L. P. Zarbo, and J. Sinova, *Phys. Rev. Lett.* **95**, 046601 (2005).
- ³¹B. A. Bernevig and S.-C. Zhang, *Phys. Rev. Lett.* **96**, 106802 (2006).
- ³²J. Wang, H. B. Sun, and D. Y. Xing, *Phys. Rev. B* **69**, 085304 (2004).
- ³³F. Mireles and G. Kirczenow, *Phys. Rev. B* **64**, 024426 (2001).
- ³⁴X. F. Wang and P. Vasilopoulos, *Phys. Rev. B* **68**, 035305 (2003).
- ³⁵X. F. Wang, *Phys. Rev. B* **69**, 035302 (2004).
- ³⁶G. Feve, W. D. Oliver, M. Aranzana, and Y. Yamamoto, *Phys. Rev. B* **66**, 155328 (2002).
- ³⁷M. Cahay and S. Bandyopadhyay, *Phys. Rev. B* **69**, 045303 (2004).
- ³⁸M. W. Wu, J. Zhou, and W. Shi, *Appl. Phys. Lett.* **85**, 1012 (2004).
- ³⁹E. G. Mishchenko and B. I. Halperin, *Phys. Rev. B* **68**, 045317 (2003).
- ⁴⁰R. M. Potok, J. A. Folk, C. M. Marcus, and V. Umansky, *Phys. Rev. Lett.* **89**, 266602 (2002).
- ⁴¹J. C. Egues, G. Burkard, and D. Loss, *Appl. Phys. Lett.* **82**, 2658 (2003).
- ⁴²S. K. Upadhyay, R. N. Louie, and R. A. Buhrman, *Appl. Phys. Lett.* **74**, 3881 (1999).
- ⁴³E. I. Rashba, *Fiz. Tverd. Tela (Leningrad)* **2**, 1224 (1960) [*Sov. Phys. Solid State* **2**, 1109 (1960)].
- ⁴⁴Y. A. Bychkov and E. I. Rashba, *J. Phys. C* **17**, 6039 (1984).
- ⁴⁵G. Dresselhaus, *Phys. Rev.* **100**, 580 (1955).
- ⁴⁶D. Sánchez, L. Serra, and M.-S. Choi, *Phys. Rev. B* **77**, 035315 (2008).
- ⁴⁷B. W. Alphenaar, K. Tsukagoshi, and M. Wagner, *J. Appl. Phys.* **89**, 6863 (2001).
- ⁴⁸C.-H. Chang, A. G. Mal'shukov, and K. A. Chao, *Phys. Rev. B* **70**, 245309 (2004).